applied sciences

MDPI

Article

Residual Properties Analysis of Steel Reinforced Recycled Aggregate Concrete Components after Exposure to Elevated Temperature

Zongping Chen [1,2,*], Rusheng Yao [1], Chenggui Jing [1] and Fan Ning [1]

1 College of Civil Engineering and Architecture, Guangxi University, Nanning 530004, China; rsy1710@163.com (R.Y.); cgj171040@163.com (C.J.); fn171040@163.com (F.N.)

2 Key Laboratory of Disaster Prevention and Structure Safety of Chinese Ministry of Education, Nanning 530004, China

* Correspondence: zpchen@gxu.edu.cn; Tel.: +86-138-7880-6048

Received: 6 October 2018; Accepted: 19 November 2018; Published: 24 November 2018

check for updates

Abstract: The application of recycled aggregate concrete (RAC) has developed rapidly in recent years. But how to evaluate the residual properties of RAC after the fires is more beneficial to the further popularization and application of RAC. This paper presents the residual properties of RAC and steel reinforced recycled aggregate concrete (SRRAC) components after exposure to elevated temperature. A total of 176 specimens (120 rectangular prisms specimens, 24 SRRAC short columns and 32 SRRAC beams) were designed and tested after exposure to elevated temperature. The parameters were considered in the test, including replacement percentage of recycled coarse aggregate (0%, 30%, 50%, 70% and 100%) and exposure to different temperatures (20, 200, 400, 600 and 800 degrees centigrade). According to the test results, heat damage and residual properties of specimens were analyzed in detail, such as surface change, mass loss, bearing capacity degradation, stiffness degradation, ductility and energy dissipation of specimens under the elevated temperature. The results showed that a series of significant physical phenomena occurred on the surface of RAC and SRRAC components after exposure to elevated temperature, such as the color changed from green-grey to gray-white, chapped on the concrete surface after 400 degrees centigrade and the mass loss of concrete is less than 10%. The degradation of mechanical properties degenerated significantly with the increase of temperature, such as the strength of RAC, and compressive capacity, bending capacity, shear capacity and stiffness of SRRAC components, among that, the degradation of the strength of RAC was most obvious, up to 26%. The ductility and energy dissipation of SRRAC components were insignificant affected by the elevated temperature. Mass loss ratio, peak deformation and bearing capacity showed a slight increase trend with the increase of replacement percentage. But the stiffness showed significant fluctuation when replacement percentage was 70% to 100%. And the ductility and energy dissipation showed significant fluctuation when replacement percentage was 30% to 70%.

Keywords: recycled aggregate concrete (RAC); steel reinforced recycled aggregate concrete (SRRAC); elevated temperature; residual properties

1. Introduction

Demolished concrete is used to make RAC, which has the advantages of being energy-saving and environment-friendly. Moreover, the steel reinforced concrete (SRC) structure has the advantages of high bearing load capacity and good seismic performance. And SRC can combined with the RAC [1–3] to form the SRRAC structure. SRRAC meets the development direction of modern architecture, which has many advantages, such as being energy-saving and environment-friendly, sustainable development, having good mechanical performance. Therefore, SRRAC has broad application prospects. However, the porosity of recycled aggregate is higher than that of natural aggregate [4]. And the coarse aggregate surface in RAC attaches the cement-based or mortar, and its initial defects are more than natural aggregate, thus, those will affect the mechanical properties of RAC [5,6]. Therefore, many studies were carried out by scholars for RAC. The results show that inferior waste concrete reduces the quality of recycled coarse aggregate and consequently reduces the strength of RAC [7]. The mechanical properties of RAC can be improved by Polyvinyl alcohol (PVA) after soaking in polyvinyl alcohol solution, which the optimum concentration of PVA solution is 10% [8]. The compressive strength of RAC increases when cement is replaced by fly ash [9]. Recycled fine aggregate with demolished concrete has little effect on the mechanical properties of RAC, when the replacement percentage is less than 30% [10]. Meanwhile, Choi, Won Chang et al. [11] conclude that the compressive strength of RAC columns meets the American Certification Institute (ACI) design criteria. Butler, L. et al. [12] consider that the bond strength of RAC is 9 to 19% lower than natural aggregate concrete. Xiao, J. et al. [13] conclude that the seismic performance of recycled concrete frame structure is reduced with the increase of replacement percentage.

Reis, Nuno et al. [14] suggest that the stiffness and cracking load of RAC slabs are slightly lower than those of natural aggregate concrete. According to the literature [15–17], the content of recycled coarse aggregate has an insignificant effect on the flexural or shear properties of RAC beams. Secondly, in order to improve the utilization ratio of RAC in high-rise and super-high-rise buildings, a large number of scholars pay attention to the structure of SRRAC. The results show that the flexural strength [18,19] and shear strength [20] of SRRAC beams are similar to those of SRC beams. SRRAC frame has good seismic performance [21], and the seismic performance of SRRAC components decreases in varying degrees with the replacement percentage of recycled aggregate increases [22–24]. The seismic performance of three beam–column joints with ordinary concrete is similar to the RAC, for which the replacement percentage of the specimens is 30% [25]. The SRRAC structure can be used in high-rise and super-high-rise buildings after reasonable preparation and design.

Fire is one of the major hazards that can affect engineering structures. It is necessary to study the fire behavior of RAC structures. The results show that the residual performance of RAC after exposure to elevated temperature is optimal level when replacement percentage is 50% [26]. The performance of RAC is similar to ordinary concrete after exposure to elevated temperature [27,28]. With the increase of elevated temperature, the elastic modulus of RAC decreases [29]. And its compressive strength increases slightly at first under the temperature of 400 degrees centigrade and then decreases with the temperature increases [30]. The ductility and cracking performance of RAC are improved after exposure to elevated temperature when the steel fibers are added [31]. Meanwhile, the energy dissipation and anti-spalling properties of RAC can improve by the rubber powder [32]. The increase of RAC strength can improve its impact behaviors when the temperature is lower than 500 degrees centigrade. RAC strength has an insignificant effect on the impact behaviors when the temperature is greater than 500 degrees centigrade [33].

In conclusion, research on the residual properties of SRRAC components after exposure to elevated temperature is limited. So that it needs to be further studied. A total of 176 specimens (120 rectangular prisms specimens, 24 SRRAC short columns and 32 SRRAC beams) were designed and tested after exposure to elevated temperature. The parameters were considered in the test, like replacement percentage of recycled coarse aggregate (0%, 30%, 50%, 70% and 100%) and exposure to different temperatures (20, 200, 400, 600 and 800 degrees centigrade). Residual properties of RAC and SRRAC were analyzed to provide reference for further research and the engineering application of SRRAC.

2. Experimental Work

A total of 176 recycled concrete specimens were designed and fabricated, including 120 rectangular prisms specimens (40 groups, three in each group), 24 SRRAC short columns and 32 SRRAC beams. The beam specimens were divided into the bending beam and the shear beam, and the corresponding shear span-to-depth ratios were 2 and 1.2, respectively. The dimensions of rectangular prisms specimens were 150 mm × 150 mm × 300 mm. Section size of SRRAC beams and columns was shown in Figure 1.

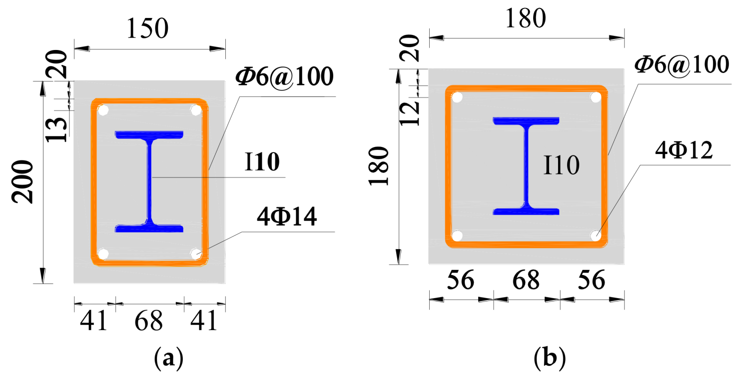

Figure 1. The section of steel reinforced recycled aggregate concrete (SRRAC) beam and column. (**a**) Beam section; (**b**) Column section.

2.1. Test Materials

All of the test materials are from Nanning, Guangxi, China. The materials were used in the test, such as 32.5R Portland cement of Guangxi conch brand, natural river sand, urban water, recycled coarse aggregate and natural gravel. Recycled coarse aggregate is derived from waste concrete specimens in laboratory, and it can be obtained after mechanical crushing, cleaning and sieving of waste concrete. Recycled and natural coarse aggregate were screened under the same conditions. Particle sizes range from 5 mm to 20 mm and continuously graded. The bulk density and water absorption ratio are 1432 kg/m^3 and 3.27%, respectively. The reference value of mix proportion design is to be r = 0%. Total mass of coarse aggregate remains constant, and only changes the ratio of recycled and natural coarse aggregate. Meanwhile, other materials remain constant. The mix proportion of concrete is shown in Table 1. Section steel is I10 of Q235. And the diameter of the stirrup bar of the columns and beams is 6 mm, and the steel bars is HPB300. The diameter of longitudinal bar (HRB335) of the columns and beams is 12 mm and 14 mm, respectively. And the detail of SRRAC beam section and column section was showed in Figure 1.

Table 1. Mix proportions of recycled concrete.

r/%	Cement/kg	Water/kg	Sand/kg	Natural Gravel/kg	Recycled Coarse Aggregate/kg
0	500	215	532	1129	0
30	500	215	532	790.3	338.7
50	500	215	532	564.5	564.5
70	500	215	532	338.7	790.3
100	500	215	532	0	1129

2.2. High-Temperature Installation and Loading System

As showed in Figure 2, RX-45-9 industrial box-type resistance furnace (Detianli Electric Furnace Manufacturer Co., Ltd., Jinan, China) was used for the high-temperature installation. And its maximum temperature can reach 950 degrees centigrade. The target temperature was set separately for batch heating based on the design of the specimen. In order to uniformly distribute the temperature inside the specimen, the temperature in high-temperature installation was constant for one hour when the furnace temperature raised to the target temperature. And then, open the furnace door and let the specimens fall to room temperature under natural conditions. The temperature in the test furnace was recorded during the test. The heating curves was showed in Figure 3. After the specimens fall to room temperature, the test block and column specimens were loaded by RMT-201 test machine

(Institute of Rock and Soil Mechanics, Chinese Academy of Sciences, Wuhan, China) which is showed in Figure 4a. Displacement control loading was adopted in the test. And the loading ratio was about 0.01 mm/s. The load-deformation curve was obtained by the acquisition system of installation. On the other hand, beam specimens were loaded by two points symmetrically. And the specimens were tested under the displacement–force mixed control. Before the pre-estimation of the ultimate load, force control was used in the test, and its step length and holding time for each level are 10 kN and 5 min, respectively. Then, when the specimen was approaching the ultimate load, displacement control loading was applied until the specimen was destroyed. And its displacement gradient was 0.5 mm. The loading installation was showed in Figure 4b.

Figure 2. High-temperature installation.

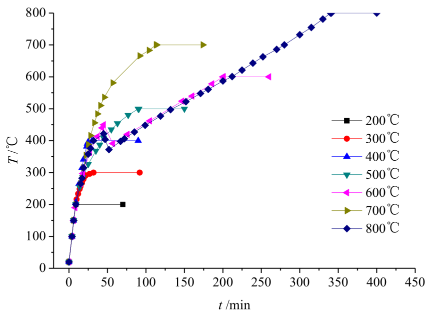

Figure 3. Heating curves.

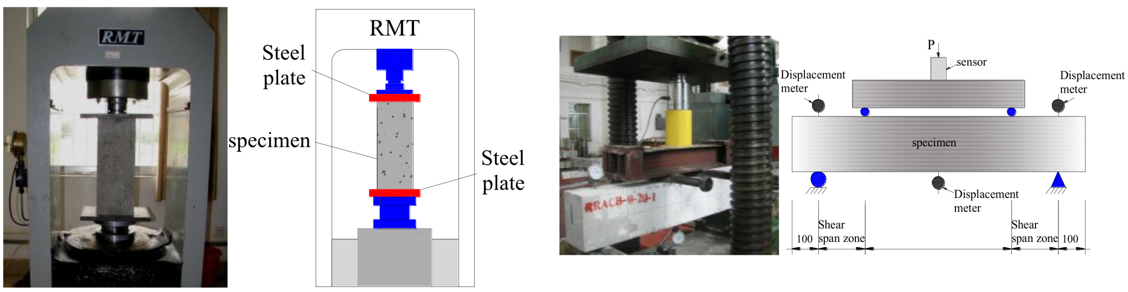

(**a**) (**b**)

Figure 4. Loading installation. (**a**) Loading installation for block and column; (**b**) Loading installation for beam.

3. Test Results

3.1. Surface Change

A series of physical and chemical reactions had occurred in recycled concrete under elevated temperature. The phenomenon (color change, cracking and spalling on concrete surface) appeared in rectangular prisms specimens, SRRAC columns and SRRAC beams. The physical phenomena of different specimens are basically similar. The color on the concrete surface changes from shallow to deeper as the temperature rises. When T is at 200 degrees centigrade to 400 degrees centigrade, the color on the concrete surface is green-grey and there are no visible cracks. And when T is at 600 degrees centigrade, the color on the concrete surface is brown-grey, and irregular micro-cracks can be found on the concrete surface. When T is at 800 degrees centigrade, the color on the concrete surface is gray-white, and the spalling phenomenon can be seen on the concrete surface. Concrete surface is green-grey due to the hydration reaction to form a little $Ca(OH)_2$. And then, the hydration products of concrete ($C_3S_2H_3$) decompose into CaO as the temperature rises, and CaO is gray-white when it contains impurities [34]. Figure 5 shows apparent morphology of rectangular prisms specimens after exposure to elevated temperature.

Figure 5. Apparent morphology of specimen after elevated temperature.

3.2. Mass Loss

The mass loss of concrete can be found at specimens after exposure to elevated temperature. Mass loss ratio (β_m) is defined to reflect this physical change. Mass loss ratio is to be $\beta_m = (M - M_T)/M \times 100\%$. And M is the mass of specimens before exposure to elevated temperature; M_T is the mass of specimens after exposure to elevated temperature.

Mass loss ratio of specimens after exposure to different elevated temperature is shown in Figure 6. As showed in Figure 6, the β_m increase as the elevated temperature increases. The β_m increases fastest when T is at 200 degrees centigrade to 400 degrees centigrade. Because the amount of water in the concrete evaporates and most of the combustible are burned at the ignition point, when the temperature reaches 200 degrees centigrade. Meanwhile, a large amount of white fog leaks out of the resistance furnace when the temperature reaches at 200 degrees centigrade to 400 degrees centigrade. This phenomenon shows that the moisture in the concrete evaporates most significant at 200 degrees centigrade to 400 degrees centigrade. Mass loss ratio of specimens grows slowly when the temperature is greater than 600 degrees centigrade. Because the moisture and combustible are completely evaporated or burned when the temperature rises to a certain extent. Therefore, mass loss ratio of specimens tends to be stable.

Figure 6d shows that the mean of β_m in each group at the same elevated temperature. According to the Figure 6d, mass loss ratio of rectangular prisms specimens increases the most significant. Mass loss ratio of SRRAC beams increase the least. Figure 6e shows that the mean of mass loss ratio of similar specimens at the same replacement percentage. According to the Figure 6e, mass loss ratio increases with replacement percentage increases. Meanwhile, mass loss ratio of replacement percentage at 100% is about 1.4 times that of the replacement percentage at 0%. Because a lot of old cement paste attach on the surface of recycled coarse aggregate. And then, more water is absorbed by the old cement paste during the stirring process. Therefore, the more recycled coarse aggregate has, the more the moisture of recycled concrete absorbs. Thus, water evaporation increased in recycled concrete after exposure to elevated temperature, and its mass loss ratio increases.

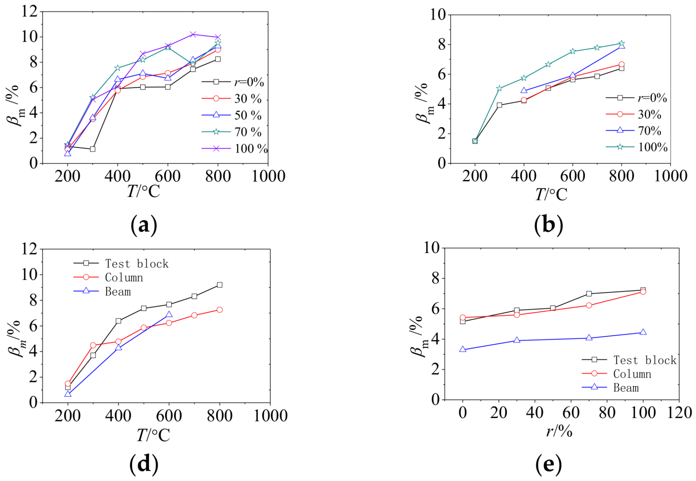

Figure 6. Mass loss ratio of specimens. (**a**) rectangular prisms specimens; (**b**) columns; (**c**) beams; (**d**) The influence of temperature on different components; (**e**) The influence of replacement percentage on different components

3.3. Failure Mode

3.3.1. Failure Mode of Rectangular Prisms Specimens

The interior of RAC has changed after exposure to elevated temperature, so that the failure process and mode of RAC are also different. The difference is more obvious with the temperature increases. The failure modes of the specimens before 400 degrees centigrade are similar to those at room temperature. These show that a few short vertical micro-cracks can be found in the middle of the specimen. As the development of stress, the cracks extend gradually toward the slope. Finally, one or two obvious oblique edge crack or crack zone is formed when the oblique edge crack penetrated specimen. After 400 degrees centigrade, the initial damage of concrete is serious due to the effect of high temperature. After the action of external force, many cracks appeared and accompanied debris falling, and a wider cracks zone is clearly visible. Typical failure modes of the specimen are shown in Figure 7 after exposure to different temperatures.

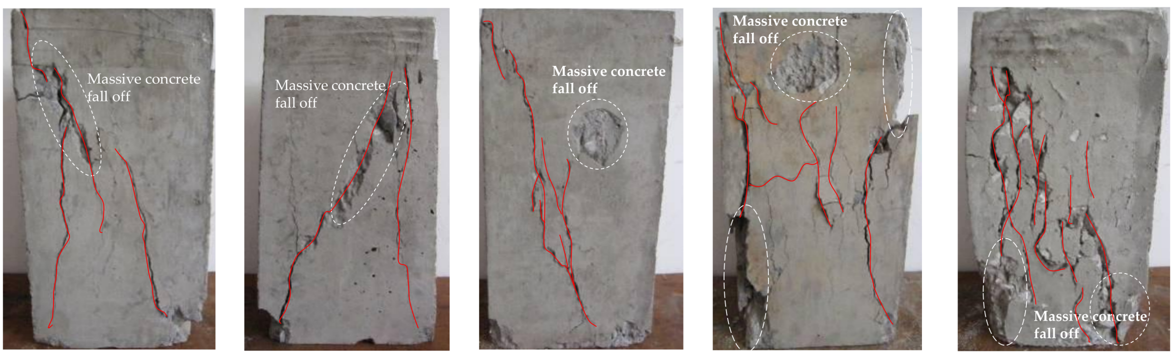

(**a**) 20 °C (**b**) 200 °C (**c**) 400 °C (**d**) 600 °C (**e**) 800 °C

Figure 7. Typical failure mode of recycled aggregate concrete (RAC).

3.3.2. Failure Mode of SRRAC Columns

It is found that the failure process and failure mode of SRRAC columns are mainly related to the highest temperature after observing the loading process of SRRAC columns under axial compression.

The failure process and mode of specimens at different replacement percentage are similar to each other at the same temperature. The failure process of specimens presents elastic stage, crack stage and failure stage. The mode and failure process of specimens after exposure to elevated temperature are as follows: The higher the temperature is, the earlier the crack appears and penetrates. The failure mechanism of the specimen is different from that of the room temperature specimen when the temperature is higher than 500 degrees centigrade. It is not the crushing failure of edge concrete. But the concrete cover falls off, then SRRAC columns damage in advance before reaching the peak load. The higher the temperature is, the earlier the concrete falls off. The failure modes of the specimen are shown in Figure 8.

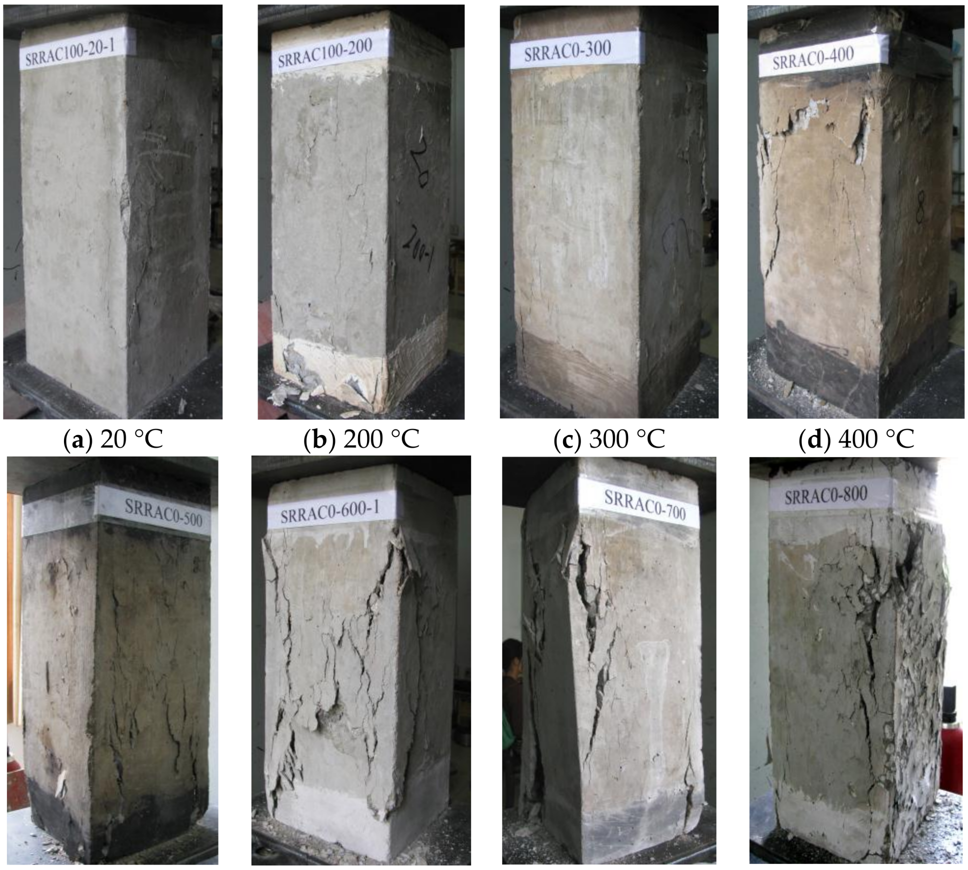

(**a**) 20 °C (**b**) 200 °C (**c**) 300 °C (**d**) 400 °C

(**e**) 500 °C (**f**) 600 °C (**g**) 700 °C (**h**) 800 °C

Figure 8. The failure modes of column specimen.

3.3.3. Failure Mode of SRRAC Beams

Failure modes of SRRAC beams after exposure to elevated temperature is the same as those at room temperature, which reflects shear-baroclinic failure, bond failure and bending failure. SRRAC beams with shear span-to-depth ratios of 1.2 show shear-baroclinic failure. SRRAC beams with shear span-to-depth ratios of 2.0 show shear-baroclinic, bond failure and bending failure.

Shear-baroclinic failure is as follows: Vertical cracks can be seen in the mid span and develop slowly upward when the external load is between 0.13 Pu and 0.35 Pu. The oblique crack appears between the loading point and the support when the external load is between 0.3 Pu and 0.6 Pu. And then, oblique cracks increase and widen, the oblique concrete zones crushed, then the specimens were destroyed.

The bending failure process is as follows: Vertical cracks can be seen in the mid span when the external load is between 0.23 Pu and 0.3 Pu. And vertical cracks increase and developed when the external load is between 0.45 Pu and 0.5 Pu. The oblique crack appears between the loading point and the support when the external load is between 0.5 Pu and 0.6 Pu. Vertical cracks develop faster when the external load is at 0.75 Pu. Finally, the concrete is crushed, then the specimen is destroyed.

Bond failure process is as follows: Longitudinal bonding crack was found near the compressive zone of section steel on the outside flange when the external load is at 0.65 Pu. Finally, the concrete to the outside of the bonding crack is split, then the specimen is destroyed. The failure modes of some specimens are shown in Figure 9. The BBi-j, SAi-j and SBi-j are used to represent corresponding pictures. And SA is shearing beam, and its span-to-depth ratio is 2.0; BB mean bending beam, and its span-to-depth ratio is 1.2. And *i* and *j* are replacement percentage and temperature, respectively.

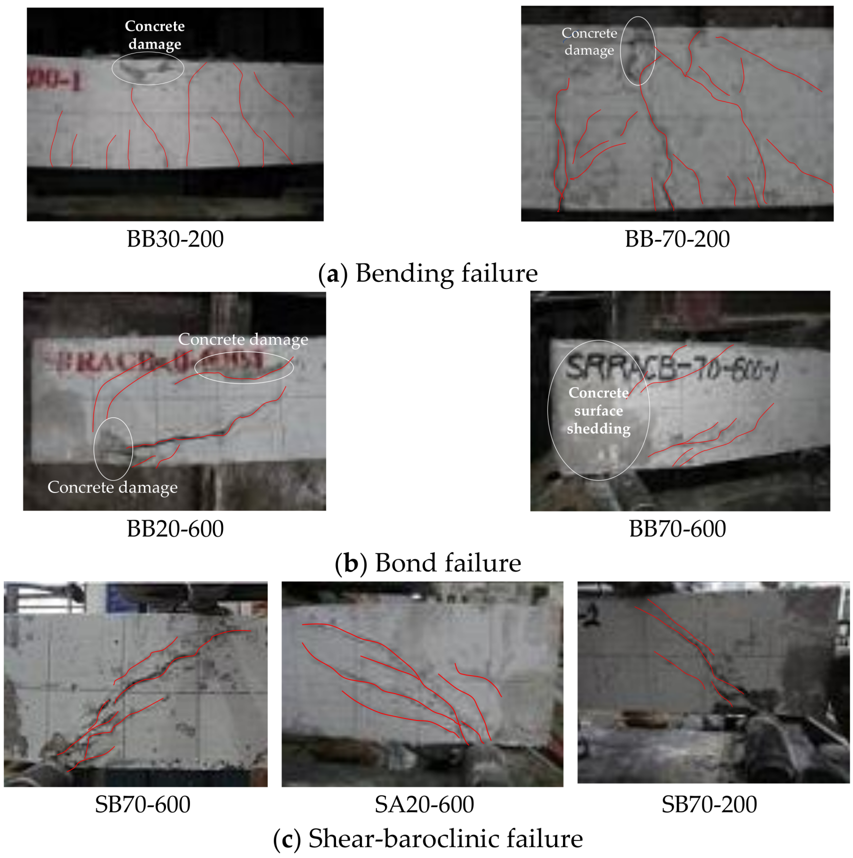

Figure 9. The failure modes of beam specimens.

3.4. Load-Displacement Curve Analysis

3.4.1. Load-Displacement Curve of Rectangular Prisms Specimens

Load-displacement curves of RAC test block was showed in Figure 10. The data in Figure 10 are the mean values of three identical test blocks in each group. According to Figure 10, the shape of the load-displacement curve of RAC exposure to elevated temperature is similar to that of ordinary concrete. And with the increase of temperature, the peak load of the curve decreases gradually, the peak displacement increases gradually, the descending stage of the curve becomes gentle and the whole curve becomes more and more flat. The effect of temperature on peak load is more and more significant when replacement percentage increases. Specimens in the elastic stage are no crack in the concrete surface, then, the specimens were brittle failure after the load exceeds the elastic limit. The peak displacement gradually increases as the temperature rises. The maximum peak displacement of RAC reaches 3.5 mm when the temperature is 800 degrees centigrade.

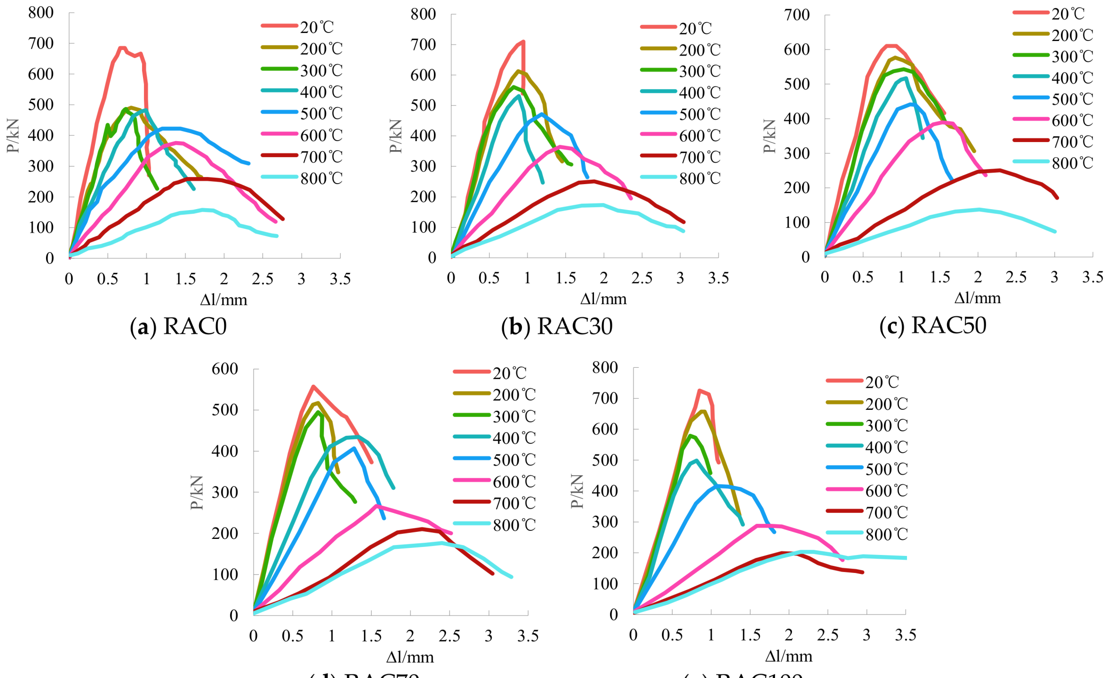

(**a**) RAC0 (**b**) RAC30 (**c**) RAC50 (**d**) RAC70 (**e**) RAC100

Figure 10. Load-displacement curve of rectangular prisms specimens.

3.4.2. Load-Displacement Curve of SRRAC Columns

According to Figure 11, as the temperature increase, the axial load-displacement curve of the SRRAC columns tends to be flat, and the value of the peak point gradually decreases. Loading process of SRRAC columns mainly includes elastic stage, elastic–plastic stage, stiffness strengthening stage, descending stage and residual stage. The characteristics of each stage are as follows:

During the elastic stage, the elastic deformation of the section steel and concrete is coordinated, and there is no crack in the concrete surface.

The elastic–plastic stage of specimens is as follows: The cracks on the concrete surface emerge and develop continuously after the load exceeds the elastic limit. And then, section steel and longitudinal reinforcement yield gradually. The load-displacement curve at this stage is nonlinear. And bond cracks appear at this stage, therefore, the bond slip between section steel and concrete is more obvious.

The stiffness strengthening stage of specimens is as follows: The load-displacement curve of the specimen appears obvious curvature rising stage before reaching the elastic limit when the exposure temperature of specimen is greater than 600 degrees centigrade. Because the evaporation of free water in the internal void of concrete makes the concrete loose. The loose concrete becomes dense with the increase of compressive load during the loading process. Therefore, the stiffness of the specimen has been improved.

During the descending stage of specimens, the bearing capacity of the specimen decreases obviously after exceeding the limit load.

The residual stage of specimens is as follows: The load decreases gently with the increase of displacement. The longitudinal reinforcement and concrete cover have basically not provided bearing capacity at all. Residual strength is provided by section steel and core-concrete.

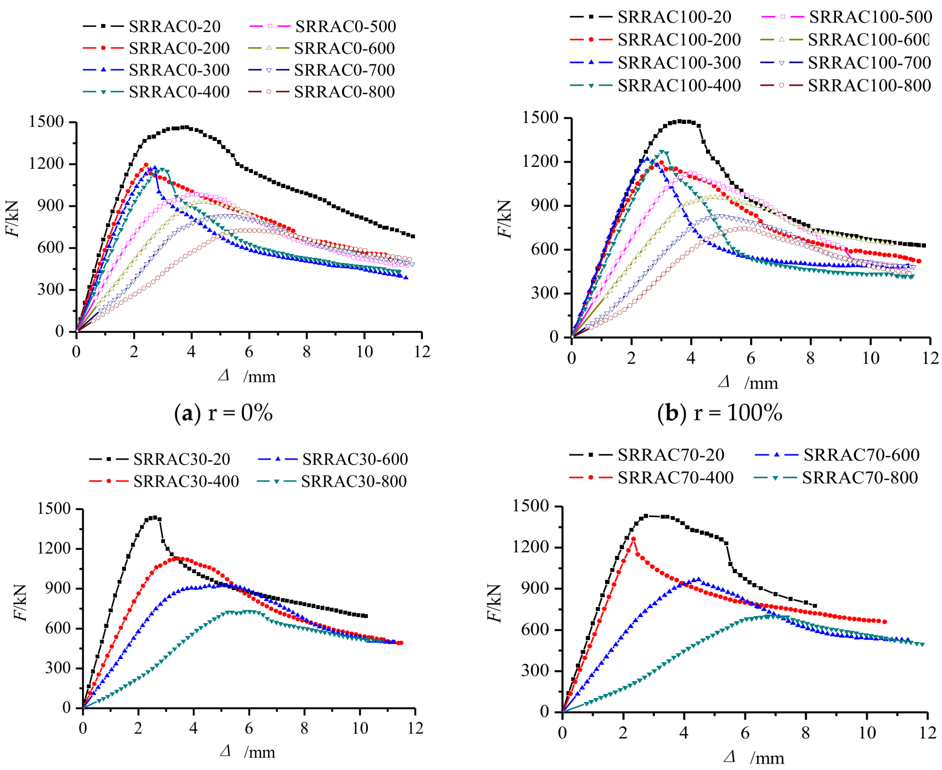

(**a**) r = 0% (**b**) r = 100%

(**c**) r = 30% (**d**) r = 70%

Figure 11. Load-displacement curve of SRRAC columns.

3.4.3. Load-Deflection Curve of SRRAC Beams

The measured load-deflection curve of SRRAC beams is showed in Figure 12. According to the Figure 12, SRRAC beams have undergone three stages: elastic stage, elastic–plastic stage and failure stage. Early loading of SRRAC beams is elastic stage. And it is elastic–plastic stage after cracking. Then, the specimen experienced the failure stage after the peak load.

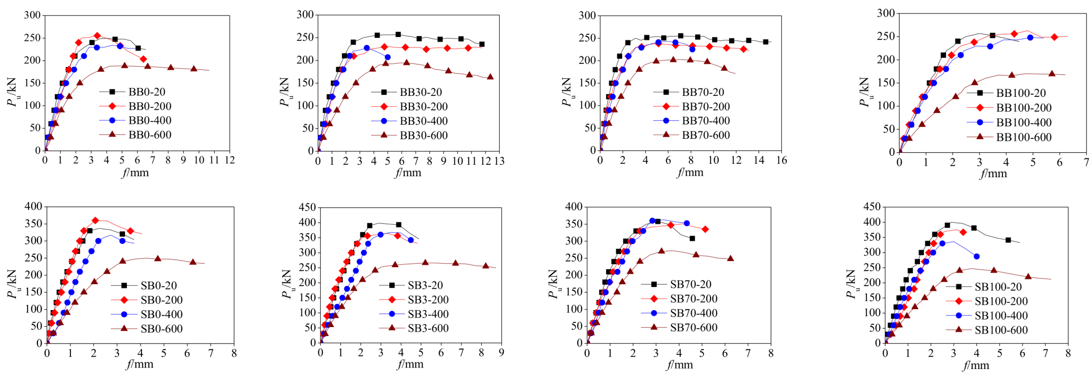

Figure 12. Load–deflection curves.

4. Residual Properties Analysis

In order to analyze the residual properties of RAC and SRRAC components after exposure to elevated temperature, many mechanical performance parameters can be obtained by the load-displacement curve of RAC and SRRAC components, such as bearing capacity, peak deformation, secant stiffness, displacement ductility factors and energy dissipation factor.

The mean performance index of all specimens is obtained at the same temperature and different replacement percentage for comparative analysis the residual properties of different components. And residual properties coefficient (β_N, β_Δ, β_K, β_μ and β_η) can be calculated by normalization based on a performance index at room temperature. Similarly, replacement percentage coefficient (α_N, α_Δ, α_K, α_μ and α_η) can be calculated by normalization based on replacement percentage at 0%.

4.1. Bearing Capacity Degradation

Figure 13 shows the degradation on bearing capacity of specimens after exposure to different elevated temperature. As seen from Figure 13a–d, compressive strength of test blocks after high temperature is deeply downtrend as the temperature ascend. The bearing capacity decreases by about 18% in the scope from 200 degrees centigrade to 400 degrees centigrade. And bearing capacity decreases by 48% when exposure to elevated temperature is at 600 degrees centigrade. Meanwhile, bearing capacity decreased by 74% when exposure to elevated temperature is at 800 degrees centigrade.

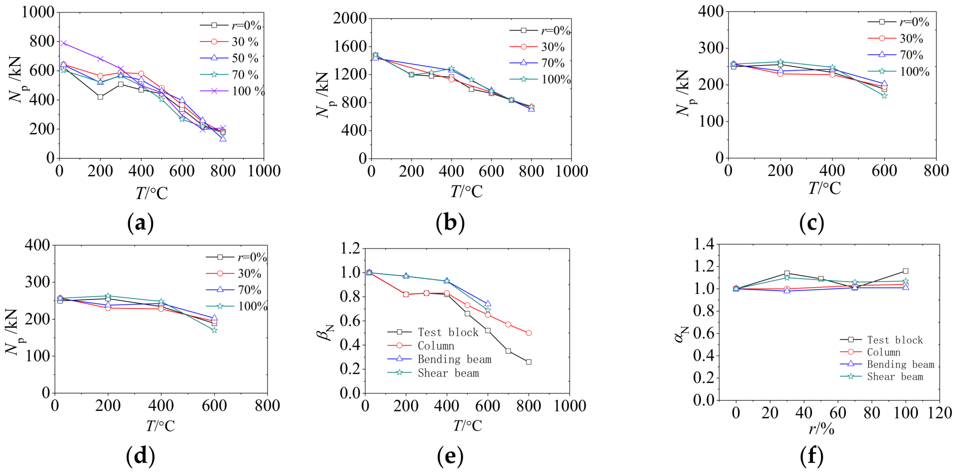

Figure 13. Bearing capacity degradation. (**a**) rectangular prisms specimens; (**b**) columns; (**c**) bending beams; (**d**) shear beams; (**e**) The influence of temperature; (**f**) The influence of replacement percentage.

After exposure to elevated temperature, the evaporation of free water and bound water in concrete leads to internal cracks. And then, the structure of hardened cement paste is crisp pine. The thermal performance of the coarse aggregate and concrete is inconsistent. Therefore, internal cracks continue to develop due to uncoordinated thermal expansion and syneresis micro-deformation. And then, the interface between aggregate and cement paste is further loosened when the temperature is above 700 degrees centigrade. Then, the pore size of cement slurry increases further. The crack between aggregate and slurry expands rapidly, the crack width increases. Therefore, the strength of concrete decreases. It can be proved by the scanning electron microscope (SEM) test in the literature [35].

As seen from Figure 13e, the bearing capacity of SRRAC components decreases significantly, especially with higher exposure to elevated temperature. However, the amplitude of reduction is slower than the test block. The law of bearing capacity degradation of the bending beam and the shear beam is basically the same. The bearing capacity is degraded slowly when T is less than 400 degrees centigrade. The degradation rate speeds up when T is greater than 400 degrees centigrade. Bearing capacity degradation rate is about 30% when T is 600 degrees centigrade. Its value is equaled to 50% of the rectangular prism specimens. The law of bearing capacity degradation of SRRAC columns under compression is similar to the prism block. And the degradation rate of SRRAC column is slower than that of rectangular prisms specimens, when T is greater than 400 degrees centigrade. The bearing capacity degradation of compression components is more serious than that of flexural components after exposure to the same elevated temperature. The β_N of compressive components is about 11%

to 22% smaller than that of flexural components in the scope from 200 degrees centigrade to 600 degrees centigrade.

As seen from Figure 13f, the replacement percentage of recycled coarse aggregate has an insignificant effect on RAC test blocks and SRRAC components after exposure to elevated temperature. As the increase of replacement percentage, the variation ranges of the bearing capacity of prism test block, compression column, bending beam and shear beam are 1~16%, 1~4%, 2~1% and 6~10%, respectively. Generally speaking, the bearing capacity of specimens increases slightly with the increase in the replacement percentage. Free water in concrete evaporates at elevated temperature action to form pore. And then, the bearing capacity of concrete falls. However, the surface of recycled coarse aggregate is rough and porous, which can hold water firmly and reduce the evaporation of free water. So bearing capacity of RAC degenerates slower than ordinary concrete. In conclusion, after exposure to elevated temperature, the bearing capacity of SRRAC components is slightly better than that of ordinary steel reinforced concrete components.

4.2. Stiffness Degradation

The law of secant stiffness degradation of specimens is shown in Figure 14. And secant stiffness is the secant modulus at 0.4 Np. As seen from Figure 14a–e, the laws of stiffness degradation of the specimens are similar to that of bearing capacity. But the degradation of stiffness is larger than that of bearing capacity. The bending stiffness of the beam deteriorated most slowly. Bending stiffness degradation rate is about 49%, when T is 600 degrees centigrade. The axial compressive stiffness of the prism test block deteriorated most rapidly. The axial compressive stiffness degradation rate is about 70% when T is 600 degrees centigrade. And the axial compressive stiffness degradation rate is about 88% when T is 800 degrees centigrade. According to the degradation trend, the stiffness degradation rate of SRRAC components under axial compression is larger than that of the flexural components after exposure to elevated temperature. Stiffness degradation coefficient (β_K) of compression components is about 5~21% less than that of the flexural member when T is at 200 degrees centigrade to 600 degrees centigrade.

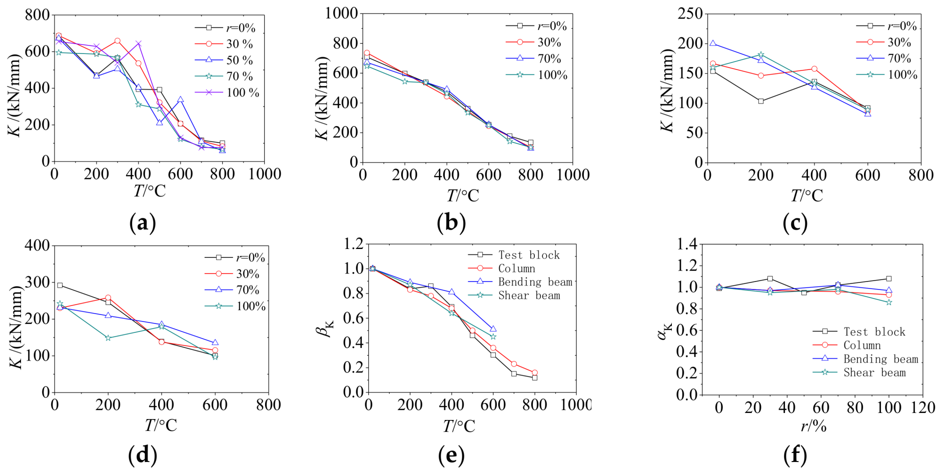

Figure 14. Stiffness degradation. (**a**) rectangular prisms specimens; (**b**) columns; (**c**) bending beams; (**d**) shear beams; (**e**) The influence of temperature; (**f**) The influence of replacement percentage.

As seen in Figure 14f, the stiffness of each component after exposure to elevated temperature is an insignificantly affected by the replacement percentage. As replacement percentage increases, the variation ranges of the axial compression stiffness of prism test block and column, flexural rigidity and shear rigidity of beams are −5~8%, −7~−3%, −3~2% and −14~−2%, respectively. In general, stiffness of a component has a slight descent trend after exposure to elevated temperature with replacement percentage increases. The cause of stiffness degradation of RAC and SRRAC is similar to that of bearing capacity degradation. Both are caused by the evaporation of free water in RAC and bond failure between the cement slurry and aggregate. And the failure mechanism of the RAC after exposure to elevated temperature is basically similar to that of ordinary concrete.

4.3. Peak Deformation

The law of peak deformation of specimens is shown in Figure 15. The peak deformation is the axial deformation corresponding to the peak load for test blocks and columns or the mid span deflection corresponding to the peak load for beams. As seen from Figure 15, peak deformation is insignificant affected by high temperature when T is less than or equal to 400 degrees centigrade. The peak deformation of the test block, column and shear beam increases rapidly with temperature increases when T is higher than 400 degrees centigrade. The peak deformation of the test block is about 2.26 times that of the room temperature. But the peak deformation of bending beams is less affected by temperature. Its peak deformation is approximately 1.24 times that of the room temperature when T is equal to 600 degrees centigrade. The increase of peak deformation is related to the increase of porosity inside concrete after exposure to elevated temperature.

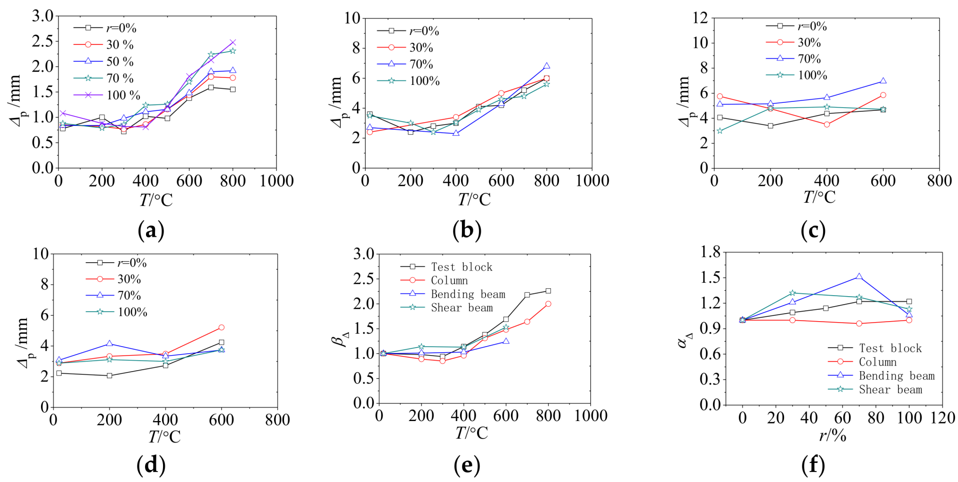

Figure 15. Deformation corresponding to the peak load. (**a**) rectangular prisms specimens; (**b**) columns; (**c**) bending beams; (**d**) shear beams; (**e**) The influence of temperature; (**f**) The influence of replacement percentage.

According to Figure 15f, the effect of replacement percentage on peak deformation of different components is different. The peak deformation linearly increases as the replacement percentage increases for a test block. And when the replacement percentage is 100%, the peak deformation is about 1.22 times that of replacement percentage at 0%. The peak deformation of the bending beams and shear beams increases first and then decreases. And those maximum increment is 39% and 32%, respectively. However, the replacement percentage has an insignificant effect on the peak deformation of axial compression column. And its peak deformation only decreases by 4% when the replacement percentage is 70%.

4.4. Ductility

Ductility ($\mu = \Delta_u/\Delta_y$) is calculated according to the load-deformation curve. And Δu is the value of deflection at 0.85 times Np, and the maximum deformation is taken to be Δu when the load falls below 0.85 Np. Δ_y is the value of initial yield deformation and calculated by the equivalent energy method. As shown in Figure 16, the dimension of OAB is equal to the dimension of YUB.

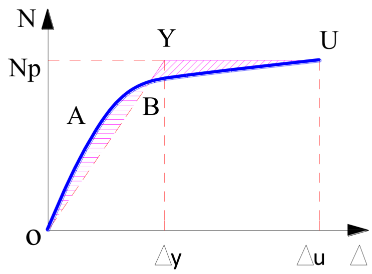

Figure 16. The sketch of energy equivalent method.

Figure 17 shows the displacement ductility factor of each component after exposure to different elevated temperature. As seen from Figure 17a–e, the displacement ductility coefficient of each component fluctuated slightly up or down as exposure to elevated temperature rises. Generally speaking, the ductility factor of the four types specimens decreases with increasing temperature when T is between 200 degrees centigrade and 400 degrees centigrade. When T is equal to 400 degrees centigrade, the displacement ductility factor of test block, column, bending beam and shear beam decrease by 10%, 28%, 44% and 31%, respectively. The displacement ductility factor of each component varies from −25% to 4% when T is higher than 400 degrees centigrade.

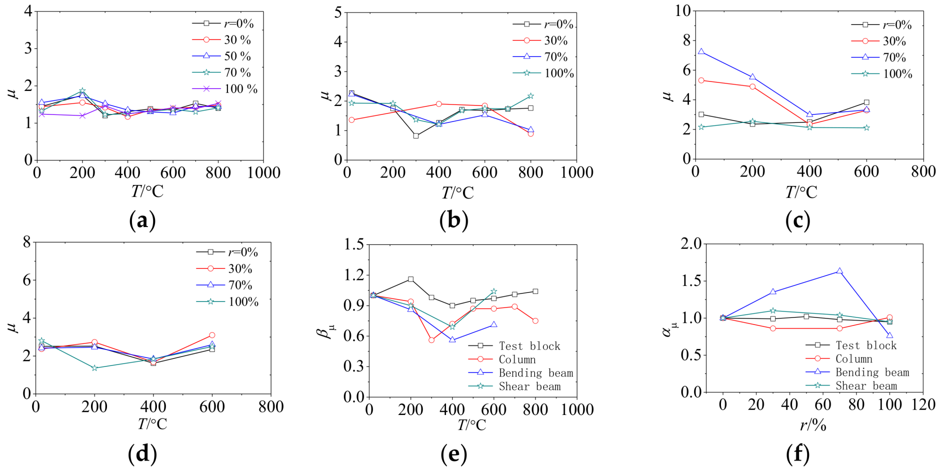

Figure 17. Ductility. (**a**) rectangular prisms specimens; (**b**) columns; (**c**) bending beams; (**d**) shear beams; (**e**) The influence of temperature; (**f**) The influence of replacement percentage.

As seen from Figure 17f, the displacement ductility factor of the bending beam increases first and then decreases. And the displacement ductility factor of bending beam increases 63% when the replacement percentage is 70%. And the displacement ductility factor of bending beam decreases 24% when replacement percentage is 100%. Then, the displacement ductility factor of the other three types of components varies slightly with replacement percentage varies.

4.5. Energy Dissipation

Energy dissipation factors ($\eta = S_{\mathrm{OUYC}}/S_{\mathrm{OABC}}$) are calculated according to the load-deformation curve. As showed in the Figure 18, the S_{OUYC} is equal to the shadow area surrounded by the load deflection curve. The S_{OABC} is equal to the rectangle area, which is passes through the peak point (U) and the limit deformation point (Y).

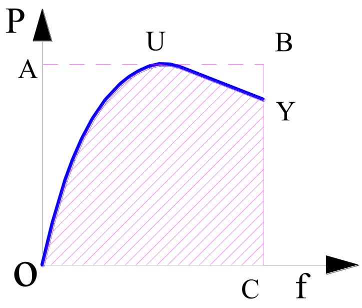

Figure 18. The sketch of energy consumption coefficient.

Figure 19 shows the energy dissipation factors of each component after exposure to different elevated temperature. As seen from Figure 19a–e, the law of energy dissipation factors of each component is similar to that of ductility factor. Energy dissipation factor decreases with the increase of temperature when T is lower than or equal to 400 degrees centigrade. When T is equal to 400 degrees centigrade, the energy dissipation factor of test block, column, bending beam and shear beam decrease by 13%, 11%, 7% and 10%, respectively. The energy dissipation factor increases slightly when T is from 400 degrees centigrade to 600 degrees centigrade. The energy dissipation factor decreases steeply when T is above 600 degrees centigrade. When T is equal to 800 degrees centigrade, the energy dissipation factor of test block and column decreases 36% and 10%, respectively. As seen from Figure 19f, the energy dissipation factor of each component is not obviously affected by the replacement percentage. The energy dissipation factor varies from −10% to 16% with replacement percentage increases.

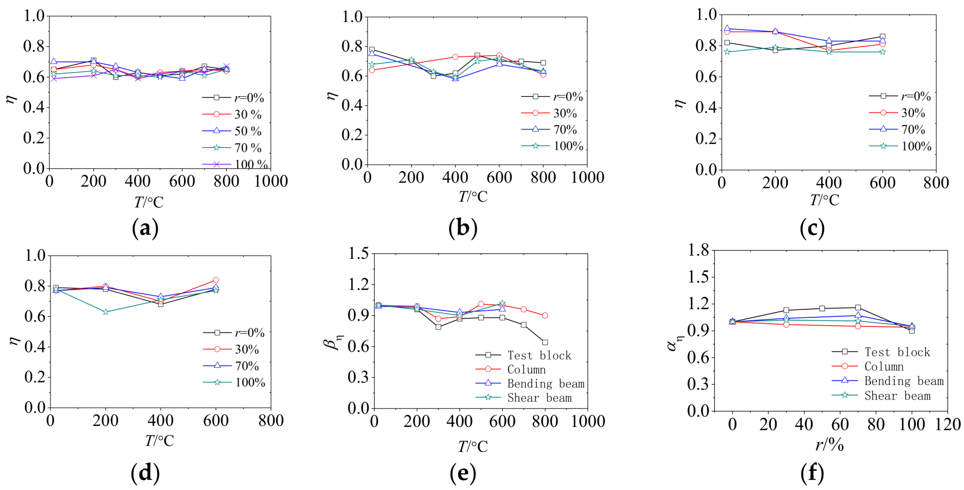

Figure 19. Energy dissipation. (**a**) rectangular prisms specimens; (**b**) columns; (**c**) bending beams; (**d**) shear beams; (**e**) The influence of temperature; (**f**) The influence of replacement percentage.

5. Conclusions

(1) Significant physical changes occurred on RAC surface after exposure to elevated temperature. Firstly, color on RAC surface changed from green-grey to gray-white. And then, chapped phenomenon occurs on the RAC surface when the temperature reached 600 degrees centigrade. Finally, the spalling phenomenon occurs on RAC surface when the temperature reaches 800 degrees centigrade. The phenomenon of mass loss can be found in the RAC after exposure to elevated temperature, and the phenomenon is more significant when the temperature and the replacement percentage increase.

(2) Mechanical properties of RAC test blocks and SRRAC components are significantly degraded after exposure to elevated temperature. And its bearing capacity and stiffness degrade most

obviously. And the performance of the prism test block degraded faster than SRRAC components. Performance degradation of SRRAC beams is slower than RAC test blocks and SRRAC columns.

(3) The bearing capacity, stiffness and peak deformation vary slightly with temperature changes when the temperature is below 400 degrees centigrade. When the temperature exceeds 400 degrees centigrade, the bearing capacity and stiffness decrease steeply, and the peak deformation increases steeply. And ductility and energy dissipation are insignificant affected by elevated temperature.

(4) Loss on ignition of specimen mass, the peak deformation and bearing capacity increase slightly with replacement percentage increases. The stiffness was significant fluctuation when replacement percentage was 70% to 100%. The ductility and energy dissipation were significant fluctuation when replacement percentage was 30% to 70%.

6. Future Research

At present, research on residual properties of SRRAC after exposure to elevated temperature is still in the initial stage. In order to further promote the application of SRRAC components, the following focuses should be further studied or discussed.

(1) This research focuses on the influence of the parameters (replacement percentage of recycled coarse aggregate and exposure to different temperatures) on the residual properties of SRRAC components. However, the coverage of steel bars or steel profiles can be influence on the mechanical properties of SRRAC components according to the regulations. Therefore, the influence of concrete cover and the coverage of steel bars or steel profiles on the residual properties of SRRAC components should be further discussed.

(2) In this research, in order to ensure the same water–cement ratio of natural aggregate concrete and recycled aggregate concrete, the same amounts of water were used in the mix proportion. However, the porosity of recycled aggregate is higher than that of natural aggregate. So that the water absorption of recycled aggregate is higher than that of natural aggregate. Therefore, in order to get more accurate test results, it is necessary to further consider the influence of the water absorption of recycled coarse aggregate on effective water cement ratio.

(3) In order to obtain more comprehensive laws of residual properties of SRRAC components after exposure to elevated temperature, the X-ray diffraction (XRD), thermogravimetric analysis (TGA) and SEM tests should be carried out for further research. Because XRD and TGA tests can reveal the chemical changes produced by the high temperatures in the concrete. And SEM tests and image analysis can identify on a microscopic scale the original, difference and failure procedures presented by the different samples.

Author Contributions: Z.C. conceived the experiments, C.J. and R.Y. designed the experiments and wrote the initial draft of the manuscript. Z.C., R.Y., C.J. and F.N. analyzed the date and wrote the final manuscript.

Funding: This research was funded by the National Natural Science Foundation of China (grant 51578163), and the project of Natural Science Foundation of Guangxi Province (2016GXNSFDA380032). And High-Level Innovation Group and Outstanding Scholar Program Project of Guangxi High Education (No. [2017]38). The authors are grateful for the above supporters.

Acknowledgments: Thanks for Yi. Li's help in the experiment.

Conflicts of Interest: The authors declare no conflict of interest.

References

1. Chen, Z.; Zhang, Y.; Chen, J.; Fan, J. Sensitivity Factors Analysis on the Compressive Strength and Flexural Strength of Recycled Aggregate Infill Wall Materials. *Appl. Sci.* **2018**, *8*, 1090. [CrossRef]
2. Oikonomou, N. Recycled concrete aggregates. *Cem. Concr. Compos.* **2005**, *27*, 315–318. [CrossRef]
3. Dhir, R.K.; Henderson, N.A.; Limbachiya, M.C. Sustainable Construction: Use of recycled concrete aggregate. *Adv. Struct. Eng.* **1998**, *11*, 383–396.

4. Gómez-Soberón, J.M.V. Porosity of recycled concrete with substitution of recycled concrete aggregate: An experimental study. *Cem. Concr. Res.* **2002**, *32*, 1301–1311. [CrossRef]
5. Loo, Y.H.; Tam, C.T.; Ravindrarajah, R.S. Recycled concrete as fine and coarse aggregate in concrete. *Mag. Concr. Res.* **1987**, *39*, 214–220.
6. Abbas, A.; Fathifazl, G.; Fournier, B.; Isgor, O.B.; Zavadil, R.; Razaqpur, A.G.; Foo, S. Quantification of the residual mortar content in recycled concrete aggregates by image analysis. *Mater. Charact.* **2009**, *60*, 716–728. [CrossRef]
7. Tam, V.W.; Wang, K.; Tam, C.M. Assessing relationships among properties of demolished concrete, recycled aggregate and recycled aggregate concrete using regression analysis. *J. Hazard. Mater.* **2008**, *152*, 703–714. [CrossRef] [PubMed]
8. Kou, S.C.; Poon, C.S. Properties of concrete prepared with PVA-impregnated recycled concrete aggregates. *Cem. Concr. Compos.* **2010**, *32*, 649–654. [CrossRef]
9. Hansen, T.C. Recycled concrete aggregate and fly ash produce concrete without portland cement. *Cem. Concr. Res.* **1990**, *20*, 355–356. [CrossRef]
10. Evangelista, L.; Brito, J. Mechanical behaviour of concrete made with fine recycled concrete aggregates. *Cem. Concr. Compos.* **2007**, *29*, 397–401. [CrossRef]
11. Choi, W.C.; Yun, H.D. Compressive behavior of reinforced concrete columns with recycled aggregate under uniaxial loading. *Eng. Struct.* **2012**, *41*, 285–293. [CrossRef]
12. Butler, L.; West, J.S.; Tighe, S.L. The effect of recycled concrete aggregate properties on the bond strength between RCA concrete and steel reinforcement. *Cem. Concr. Res.* **2011**, *41*, 1037–1049. [CrossRef]
13. Xiao, J.; Sun, Y.; Falkner, H. Seismic performance of frame structures with recycled aggregate concrete. *Eng. Struct.* **2006**, *28*, 1–8. [CrossRef]
14. Reis, N.; Brito, J.D.; Correia, J.R.; Arruda, M.R.T. Punching behaviour of concrete slabs incorporating coarse recycled concrete aggregates. *Eng. Struct.* **2015**, *100*, 238–248. [CrossRef]
15. Knaack, A.M.; Kurama, Y.C. Behavior of Reinforced Concrete Beams with Recycled Concrete Coarse Aggregates. *J. Struct. Eng.* **2015**, *141*, B4014009. [CrossRef]
16. Ev, M.M.; Radonjanin, V.; Marinkovi, S.A. Recycled Concrete as Aggregate for Structural Concrete Production. *Sustainability* **2010**, *2*, 1204–1225.
17. Fathifazl, G.; Razaqpur, A.G.; Isgor, O.B.; Abbas, A.; Fournier, B.; Foo, S. Shear capacity evaluation of steel reinforced recycled concrete (RRC) beams. *Eng. Struct.* **2011**, *33*, 1025–1033. [CrossRef]
18. Jia, Y.D.; Guo, Y.K.; Sun, Z.P.; Zhao, X. Experimental Research on Behavior of Composite Beams of Steel-Reinforced Recycled Concrete. *Adv. Mater. Res.* **2013**, *639–640*, 145–148. [CrossRef]
19. Fathifazl, G.; Razaqpur, A.G.; Isgor, O.B.; Abbas, A.; Fournier, B.; Foo, S. Flexural Performance of Steel-Reinforced Recycled Concrete Beams. *ACI Struct. J.* **2009**, *106*, 858–867.
20. Fathifazl, G. *Structural Performance of Steel Reinforced Recycled Concrete Components*; Dissertation Abstracts International; Carleton University: Ottawa, ON, Canada, 2008; Volume 69, p. 1175.
21. Xue, J.; Zhang, X.; Ren, R.; Zhai, L.; Ma, L. Experimental and numerical study on seismic performance of steel reinforced recycled concrete frame structure under low-cyclic reversed loading. *Adv. Struct. Eng.* **2018**, *21*, 1895–1910. [CrossRef]
22. Ma, H.; Xue, J.; Liu, Y.; Zhang, X. Cyclic loading tests and shear strength of steel reinforced recycled concrete short columns. *Eng. Struct.* **2015**, *92*, 55–68. [CrossRef]
23. Xue, J.; Zhai, L.; Bao, Y.; Ren, R.; Zhang, X. Seismic behavior of steel-reinforced recycled concrete inner-beam-column connection under low cyclic loads. *Adv. Struct. Eng.* **2017**, *21*, 631–642. [CrossRef]
24. Ma, H.; Xue, J.; Zhang, X.; Luo, D. Seismic performance of steel-reinforced recycled concrete columns under low cyclic loads. *Constr. Build. Mater.* **2013**, *48*, 229–237. [CrossRef]
25. Gonzalez, V.C.L.; Moriconi, G. The influence of recycled concrete aggregates on the behavior of beam–column joints under cyclic loading. *Eng. Struct.* **2014**, *60*, 148–154. [CrossRef]
26. Govinda, G.G.; Rao, B.S.; Naik, S.M. Behaviour of Recycled Aggregate Concrete on exposed to Elevated Temperature. *Int. J. Civ. Eng.* **2017**, *4*, 5–13.
27. Salau, M.A.; Oseafiana, O.J.; Oyegoke, T.O. Effects of Elevated Temperature on Concrete with Recycled Coarse Aggregates. In *IOP Conference Series: Materials Science and Engineering*; IOP Publishing: Bristol, UK, 2015; Volume 96, p. 012078.

28. Laneyrie, C.; Beaucour, A.L.; Green, M.F.; Hebert, R.L.; Ledesert, B.; Noumowe, A. Influence of recycled coarse aggregates on normal and high performance concrete subjected to elevated temperatures. *Constr. Build. Mater.* **2016**, *111*, 368–378. [CrossRef]
29. Gupta, A.; Mandal, S.; Ghosh, S. Recycled aggregate concrete exposed to elevated temperature. *J. Eng. Appl. Sci.* **2012**, *7*, 100–107.
30. Liu, Y.; Ji, H.; Zhang, J.; Wang, W.; Chen, Y.F. Mechanical properties of thermal insulation concrete with recycled coarse aggregates after elevated temperature exposure. *Mater. Test.* **2016**, *58*, 669–677. [CrossRef]
31. Chen, G.M.; He, Y.H.; Yang, H.; Chen, J.F.; Guo, Y.C. Compressive behavior of steel fiber reinforced recycled aggregate concrete after exposure to elevated temperatures. *Constr. Build. Mater.* **2016**, *128*, 272–286. [CrossRef]
32. Guo, Y.C.; Zhang, J.H.; Chen, G.M.; Xie, Z.H. Compressive behaviour of concrete structures incorporating recycled concrete aggregates, rubber crumb and reinforced with steel fibre, subjected to elevated temperatures. *J. Clean. Prod.* **2014**, *72*, 193–203. [CrossRef]
33. Li, W.; Luo, Z.; Wu, C.; Tam, V.W.Y.; Duan, W.H.; Shah, S.P. Experimental and numerical studies on impact behaviors of recycled aggregate concrete-filled steel tube after exposure to elevated temperature. *Mater. Des.* **2017**, *136*, 103–118. [CrossRef]
34. Gu, L.; Ling, F.; Sheng, Z. Research on properties of concrete and its compositions after high temperature. *Sichuan Build. Sci.* **1991**, *2*, 1–5. (In Chinese)
35. Zai, Q.; Hui, W. Research on Scanning Electron Microscopic of Concrete after High Temperature. *J. Fuzhou Univ.* **1996**, *S1*, 36–40. (In Chinese)